Canadian Technical Report of
Hydrography and Ocean Sciences 212

2000

Assimilating Sea Surface Temperature Data into an Ice-Ocean Model of the Labrador Sea

by

Tom Yao

Ocean Sciences Division
Maritimes Region
Fisheries and Oceans Canada

Bedford Institute of Oceanography
P.O. Box 1006
Dartmouth, Nova Scotia
Canada B2Y 4A2

Acknowledgment

This work is funded by the Panel on Energy Research and Development.

Cat. No. Fs97-18/212E ISSN:0711-6764

Correct citation for this publication:

Yao, Tom. 2000. Assimilating Sea Surface Temperature Data into an Ice-Ocean Model of the Labrador Sea. Can. Tech. Rep. Hydrogr. Ocean Sci. 212, iv + 26p.

Table of Contents

Abstract

Yao, Tom. 2000. Assimilating Sea Surface Temperature Data into an Ice-Ocean Model of the Labrador Sea. Can. Tech. Rep. Hydrogr. Ocean Sci. 212, iv + 26p.

We examine the feasibility of assimilating satellite sea surface temperature (SST) data into a numerical model of Labrador sea ice with the objective of improving ice edge location. We use statistical interpolation to derive an analysis SST field from the model surface temperature and the Oceans Pathfinder SST data set. The dominant response of sea ice is to local changes in SST, in particular to the location of SST gradients. We are unable to demonstrate improvement in ice edge location by assimilation of SST. The lack of improvement is related to the limited spatial and temporal resolution of the (present generation) satellite SST data during winter because of cloud cover. Assimilation of SST is not effective in modifying the ice edge when ice is receding.

Résumé

Yao, Tom. 2000. Assimilating Sea Surface Temperature Data into an Ice-Ocean Model of the Labrador Sea. Can. Tech. Rep. Hydrogr. Ocean Sci. 212, iv + 26p.

Nous examinons la faisabilité d'assimiler des données satellite sur la température de la mer en surface (TMS) à un modèle numérique de la glace de mer du Labrador dans le but d'améliorer la détermination de l'emplacement du front de glace. Nous utilisons une interpolation statistique pour établir un champ d'analyse de la TMS à partir de la température de surface de référence et l'ensemble de données sur la TMS d'Oceans Pathfinder. La glace de mer réagit principalement aux changements locaux de la TMS, en particulier à l'emplacement des gradients de la TMS. Nous ne pouvons pas démontrer que l'assimilation de la TMS mène à une amélioration de la détermination de l'emplacement du front de glace. L'absence d'amelélioration est due à la résolution spatiale et temporelle limitée des données satellite (de la génération actuelle) sur la TMS en hiver en raison de la couverture nuageuse. L'assimilation de la TMS ne permet pas de suivre de façon efficace l'emplacement du front de glace lorsque la glace se retire.

1. Introduction

The seasonal cycle of Labrador sea ice can be simulated with numerical models giving reasonable agreement with observations (e.g. Yao et al., 2000). It is then feasible to apply the models to produce nowcasts and forecasts of ice conditions. In such forecasts, atmospheric forcing data is derived from a numerical weather prediction model. The ocean state is initialised with climatological data. The question arises whether remotely sensed ocean data can be assimilated into the models to improve the ice forecasts. Here we consider the usefulness of sea surface temperature (SST) data derived from satellite-borne Advanced Very High Resolution Radiometer (AVHRR) sensors. The premise is that remotely sensed SST can correct the model mixed-layer temperature and directly influence the rate of ice growth or melt.

In assimilation studies of the Gulf Stream it is necessary to project surface data into the deep ocean (Ezer and Mellor, 1997). Our goal is to use SST more to modify ice thermodynamics and less to modify ocean currents. We therefore assimilate SST data into the surface of the ocean model and allow the model to adjust at depth. Our study is more in line with the approach taken by Annan and Hargreaves (1999) who assimilated SST data into a model of the North Sea. Annan and Hargreaves showed that assimilation reduced the rms error between model SST and ship-measured SST but had an extremely small effect on currents. Fischer and Latif (1995) assimilated SST data into a model of the tropical Pacific. The assimilation reduced the rms difference between model and observed SST. Over a number of years, the assimilation modified temperature below the thermocline and altered the currents.

Yao et al. (2000) demonstrated the importance of ice melt in the vicinity of the ice edge on the ice mass balance. Within the ocean, horizontal mixing of heat balanced the cooling caused by ice melt at the ice edge. These results show the importance of ocean surface temperature in the vicinity of the ice edge on the ice distribution.

2. Sea Surface Temperature Data

We have selected for this study the NOAA/NASA Oceans Pathfinder SST data (Smith et al., 1996). The Pathfinder SST is derived from AVHRR data using an algorithm improved over that of an alternative data set, the multichannel sea surface temperature (MCSST) data. The Pathfinder data is not available in near real time. For operational application, further investigation of the properties of available real-time SST would be required.

However, this study shows that there are obstacles to assimilation even without the real-time requirements.

The Pathfinder data is available in various spatial and temporal resolutions. We have chosen for this preliminary investigation the lowest resolution: monthly-averaged data at 0.5 degree resolution. We select data from the descending pass (night time data). Annan and Hargreaves (1999) report that in the North Sea the Pathfinder data showed a bias of 0.41°C and, with the bias removed, a rms error of 0.39°C when compared with direct observations. The Pathfinder data is archived at the Physical Oceanography Distributed Active Archive Center of the NASA Jet Propulsion Laboratory (http://podaac.jpl.nasa.gov).

3. Model Description

The coupled ice-ocean model used in this study is described in Yao et al. (2000). The ice component is comprised of multiple ice categories and is derived from Hibler (1979, 1980). The ocean component is the Princeton Ocean Model (Mellor, 1996 and Blumberg and Mellor, 1987). The parameterisations of heat and salt fluxes between ice and ocean are derived from Mellor and Kantha (1989). A map of the study region and the model domain is drawn in Figure 1. The model resolution is 1/6° latitude by 1/5° longitude.

The model is driven by prescribed atmospheric forcing (wind, air, temperature, and dew point). In this study the atmospheric forcing is 6-hourly data for 1996-1997 from the Canadian Meteorological Centre Regional Forecasting Model. The model integration is initiated in November with climatological ocean temperature and salinity (Tang and Wang, 1996). Ocean transport and climatological ocean temperature and salinity are prescribed at open boundaries. Ice forms locally and flows into the region from the northern boundary where ice is prescribed.

We compare model results with observed ice distribution. The observed ice consists of digitised daily ice charts prepared by the Canadian Ice Service.

4. Assimilation Methodology

The satellite SST data is irregularly distributed in space. We attempt to extract the maximum signal from the satellite SST data using statistical interpolation (e.g. Daley, 1991).

Statistical interpolation requires a background, or first-guess, field. Here the background field consists of the model SST. Let us denote $T(\mathbf{r})$ as the SST at

the spatial location $\mathbf{r}$. The data is observed at irregularly spaced points $\mathbf{r}_k$, $k = 1\ldots K$. The observed and background values at the observing location are $T_O(\mathbf{r}_k)$ and $T_B(\mathbf{r}_k)$ respectively. The background value may have to be interpolated to $\mathbf{r}_k$. We wish to define an analysis value at the gridpoint $\mathbf{r}_i$. We denote $T_A(\mathbf{r}_i)$ and $T_B(\mathbf{r}_i)$ as the analysis and background values at $\mathbf{r}_i$.

The analysis value is

$$T_A(\mathbf{r}_i) = T_B(\mathbf{r}_i) + \sum_{k=1}^{K} W_{ik}[T_O(\mathbf{r}_k) - T_B(\mathbf{r}_k)]. \tag{1}$$

The weights W_{ik} in (1) are determined by minimising the expected error in the analysis field. The minimisation results in a set of linear equations

$$\sum_{l=1}^{K} W_{il}[\rho_B(\mathbf{r}_k,\mathbf{r}_l) + \varepsilon_O^2 \rho_O(\mathbf{r}_k,\mathbf{r}_l)] = \rho_B(\mathbf{r}_k,\mathbf{r}_i) \qquad k = 1\ldots K \tag{2}$$

where $\rho_B(\mathbf{r}_k, \mathbf{r}_l)$ and $\rho_O(\mathbf{r}_k, \mathbf{r}_l)$ are the background and observation error correlation respectively between observation locations $\mathbf{r}_k$ and $\mathbf{r}_l$. On the rhs of (2) $\rho_B(\mathbf{r}_k, \mathbf{r}_i)$ is the background error correlation between grid location $\mathbf{r}_i$ and observation location $\mathbf{r}_k$. ε_O^2 is the ratio between observation error variance and background error variance (assumed to be homogeneous here). The statistical interpolation algorithm (1) and (2) results in minimum expected error if ρ_B, ρ_O, and ε_O^2 are correctly known. In the present application the number of observations K is of order 1000. The system of linear equations (2) is solved using LAPACK (Anderson et al., 1999) routines for symmetric, positive definite matrices.

The SST field along the Labrador coast is characterised by isotherms tending to align along the bathymetry with maximum gradients associated with the shelf slope. For this reason we specify an anisotropic background error correlation $\rho_B(\mathbf{r}_k, \mathbf{r}_l)$ which is dependent on bottom depth

$$\rho_B(\mathbf{r}_k,\mathbf{r}_l) = \exp\left[-\frac{|\mathbf{r}_k - \mathbf{r}_l|^2}{L^2} - \frac{(h_k - h_l)^2}{L_h^2}\right] \tag{3}$$

where h_k and h_l are bottom depths. The values selected for L, L_h and other assimilation parameters are given in Table 1.

The observation error correlation is chosen to consist of a correlated part and an uncorrelated part

$$\rho_O(\mathbf{r}_k, \mathbf{r}_l) = 0.5[\rho_B(\mathbf{r}_k, \mathbf{r}_l) + \delta_{kl}] \tag{4}$$

where δ_{kl} is the Kronecker delta.

To illustrate the statistical interpolation procedure we draw model and Pathfinder SST fields for December, 1996 in Figure 2. The model results (Figure 2a) are from the control run (no assimilation) and are an instantaneous SST field from mid-December. The Pathfinder data (Figure 2b) is the average over the month of December. SST from the control run and from the Pathfinder data are very similar. In both the model and Pathfinder data there is a sharp gradient in SST (which for brevity we shall refer to as a front) over the Labrador slope. In both the model and Pathfinder data there is cold water over the west Greenland shelf. There is general agreement in SST over the Labrador Sea.

In Figure 2 we also draw the analysis increment ($T_A - T_B$) derived from (1) to (4) using the control field (Figure 2a) as the background and the Pathfinder data (Figure 2b) as the observations. To illustrate the impact of the depth-dependent term on the background error correlation (3) we draw the analysis increment both omitting the term (Figure 2c) and including it (Figure 2d). Omitting the depth-dependent term results in a smoothed analysis increment. Including the depth-dependent term reveals structure aligned along the bathymetry. A prominent feature is the positive analysis increment around 54°N over the slope. At this location the SST front in the Pathfinder data is located inshore of the SST front in the control run. The implied shift in the SST front has an important influence on the ice edge and henceforth we retain the depth-dependent part of the background error correlation.

The analysis SST T_A derived from (1) to (4) is introduced into the model by nudging the surface temperature and allowing the model physics to adjust at depth. The nudging method has been used in ocean data assimilation by Holland and Malanotte-Rizzoli (1989) and by Malanotte-Rizzoli and Young (1992). The nudging method can be written as the addition of a nudging term to the governing equation for temperature T in the uppermost model layer

$$\frac{\partial T}{\partial t} = \text{model physics} - \frac{R}{\Delta z}(T - T_A) \tag{5}$$

where t is time, Δz is the thickness of the uppermost model layer, and R is the nudging parameter. The model physics represent the original terms in the equation: advection, diffusion, and surface heat flux. The Δz factor implies that (5) is integrated over the uppermost model layer and that for a given temperature difference ($T - T_A$) the surface heat flux equivalent to the nudging term is the same regardless of layer depth. This factor is necessary because in our sigma-coordinate system the uppermost layer thickness varies with location, depending linearly on bottom depth.

Here R is constant although, in general, it could be a function of time (for example decreasing as the interval between observation time and model time increases). Associated with the nudging parameter is a relaxation time T_e defined

$$T_e = \Delta z / R \qquad (6)$$

For a long relaxation time, the model physics dominates. For shorter relaxation times the model temperature increasingly approaches the analysis temperature.

The nudging (5) is applied every time step. An analysis field T_A is derived from (1) once a day. The matrix on the lhs of (2) is inverted whenever the observations change (once per month).

As we have previously noted, the analysis temperature nudges the uppermost model layer and the model adjusts at depth. An alternative procedure (similar to that used by Annan and Hargreaves, 1999) is to determine a depth for the mixed layer and nudge throughout the mixed layer.

Ocean temperature is constrained to be greater than or equal to the freezing temperature. The AVHRR data is unable to determine the SST in the presence of ice because of the generally lower surface temperatures of the ice. Because of these two considerations we do not nudge the ocean temperature in a model cell which contains ice. Furthermore, if T_A from (1) leads to a temperature below the freezing temperature, T_A is set to the freezing temperature.

One further step is required in the assimilation. The upper ocean in the Labrador Sea is weakly stratified. If the analysis temperature T_A is lower than the model temperature in (5), then nudging the temperature increases the surface density. The cold, dense surface water then mixes with the deeper water which is generally warmer. The mixing prevents the surface temperature from approaching the analysis temperature and the nudging term from diminishing. The mixing thus deepens. To remedy this difficulty

we determine an analysis increment for surface salinity $S_A - S_B$ which is proportional to the analysis increment for SST

$$S_A - S_B = c(T_A - T_B) \tag{7}$$

where c is a constant. We then nudge salinity using S_A and an equation analogous to (5). This is an admittedly *ad hoc* procedure which we adapt for a preliminary investigation. We suggest below that it is not a limiting factor in the assimilation.

5. Results

We first compare the model and observed seasonal cycle of ice. In Figure 3 we draw the ice extent south of 55°N during 1996-1997 from the control run, from the model run with assimilation, and from the observed ice. Ice extent is here defined as the area within the 0.1 concentration contour. Ice reaches 55°N in late December, reaches a maximum extent in March, and largely clears the latitude by May. The control run is a reasonable approximation to the observed ice extent. There are discrepancies between the control run and the observations in March, around the time of maximum extent. There are greater discrepancies during the ice retreat in April and May.

In our assimilation run we do not modify the SST beneath the ice. During retreat the ice edge recedes over a region which is previously ice covered. Thus we would not expect the assimilation of SST to have a significant effect on ice cover during the retreat phase (although assimilation could presumably have a secondary effect by modifying the previously accumulated ice or by modifying large-scale ocean heat fluxes). We focus our examination of the SST assimilation during the time of maximum ice extent in February and March.

The ice extent from the assimilation run is also drawn in Figure 3. There is little difference between the control run and the assimilation run during the advance and the retreat stages. During the February and March period the assimilation run does not agree as well as the control run with the observed ice extent. We investigate the reasons why the assimilation does not improve agreement with the observed extent.

One measure of the effect of the assimilation is the difference between model and Pathfinder SST. The rms difference for February and March is given in Table 2 for the control run and the assimilation run. For the model runs the SST field is an instantaneous mid-month field, interpolated to the locations of the monthly Pathfinder data. Table 2 shows that in February, for example,

the rms SST difference is reduced from 1.65°C for the control run to 0.96°C for the assimilation run.

5.1 February, 1997 Comparison

In Figure 4 we compare SST from the control run with Pathfinder SST for February, 1997. The SST from the control run is an instantaneous field from mid-month. The Pathfinder SST is a monthly average. The February Pathfinder data (Figure 4b) illustrates the primary difficulty with using satellite SST data in the Labrador Sea during winter. Data from the northern Labrador Sea is extremely sparse because of pervasive cloud cover. There is no SST data from ice-covered regions. In Figure 4c we draw the analysis increment in SST based on the control run (Figure 4a) as background and the Pathfinder data (Figure 4b) as observations. The analysis increment is negative over the Labrador slope north of 56°N. However given the paucity of data (Figure 4b) this feature may not be realistic. The dominant feature of the analysis is the positive increment between 48 and 55°N over the slope. The analysis will tend to shift the model SST front in the onshore direction.

In Figure 5 we draw the ice edge on 13 February 1997 for the control run, the assimilation run, and the observations. North of 56°N the effect of the assimilation is to shift the ice edge further offshore, in this case, in better agreement with the observations. South of 54°N the ice edge from the control run agrees well with the observed edge (except at the southern limit). The effect of the assimilation is to shift the model ice edge in the onshore direction, away from the observed ice edge. The shift in the ice edge is, however, consistent with the SST analysis increment (Figure 4c).

We can better visualise the relation between ice edge and SST and the effect of the assimilation by plotting cross sections of SST. In Figure 6a we draw the SST on 13 February 1997 along 58°N for the control run, the assimilation run, and the analysis field (based on the control run and the Pathfinder data). The SST front is well defined in the model runs and the analysis field. The SST front from the analysis field is offshore of the SST front in the control run by about 1 degree longitude. Assimilating SST shifts the model front offshore to the location of the analysis field. Also shown in Figure 6a is the location of the ice edge at this latitude for the control run, the assimilation run, and the observed ice. The assimilation shifts the ice edge offshore, in closer agreement with the observations.

In Figure 6b the corresponding cross-sections at 51°N are drawn. At this latitude the ice edge from the control run agrees well with the ice edge from the observations. The SST shows two frontal regions. The outer front is related to the warmer N. Atlantic current. The inner front is associated with

shelf water and the ice edge. The location of the inner front from the analysis field is inshore of the location from the control run by almost 2 degrees longitude. In the assimilation run the model SST front shifts to the analysis front and causes an onshore shift in the ice edge, in this case away from the observed ice edge.

How do we account for the poorer agreement between model and observed ice edge when SST is assimilated? The greatest difference between model and satellite SST is associated with differences in position of the SST front. This is evident in Figures 4 and 6. Moreover the ice edge responds directly to displacements of the SST front caused by assimilation. This is evident in Figures 5 and 6. High spatial and temporal resolution is required to define the position of the SST front. Apparently the winter Labrador Sea cloud coverage precludes adequate resolution of the SST front in the satellite data.

To illustrate the limits of resolution of the satellite data we show the Pathfinder SST fields for the four 8-day periods which span February 1997 in Figure 7. The sparseness of the data and the resulting difficulty in resolving the front are obvious.

In Figure 8 we draw cross sections of analysis SST (mid-February control run as background) from 58 and 51°N from the four 8-day periods. For these analysis fields we have reduced the ratio of observation to background error variance ε_O^2 from 1 to 0.1. We have also set the observation error to be uncorrelated. Both these changes will cause the analysis field to follow the SST data more closely. We also draw the location of the observed ice edge and the ice edge from the assimilation run in Figure 8.

Figure 8 shows the variability in the 8-day SST analysis fields. Part of this is temporal variability; February is a time of rapid ice expansion (Figure 3). An additional part of the variability reflects uncertainty in the analysis SST. The determination of a SST front is sensitive to the distribution of the satellite data. We assume an along-bathymetry form to the background error correlation (3). Such an assumption is necessary to resolve small-scale structure. However the assumption may not be entirely justifiable and it may lead to an analysis SST front more aligned with the bathymetry than is actually the case.

5.2 March, 1997 Comparison

We now examine the results during March, 1997. In Figure 9a we draw the instantaneous SST field from the control run in mid-March. In Figure 9b we draw the Pathfinder SST field averaged over March. The data coverage is greater than in February. Between 52°N and 58°N the SST front is clearly defined in the Pathfinder data. In Figure 9c we draw the analysis increment

in SST based on the background and observation fields of Figures 9a and 9b. Between 52 and 58°N over the slope, the lack of a pronounced feature in the analysis increment signifies agreement between the location of the analysis front and the model front.

In Figure 10 we draw the ice edge on 16 March 1997 for the control run, the assimilation run, and the observed ice. Between 52 and 58°N the observed ice edge is offshore of the ice edge from the control run; assimilation of SST has little effect on ice edge in this latitude range.

Again, to better visualise the relationship between ice edge and SST front, in Figure 11 we draw cross-sections of SST temperature on 16 March 1997 for the control run, the assimilation run, and the analysis (based on the control run and the March Pathfinder data). Also drawn are the locations of the ice edge in the control run, the assimilation run, and the observed ice The cross-sections are for 56°N (Figure 11a) and 53°N (Figure 11b). At each latitude the SST from the control run agrees well with the analysis SST; assimilation has little effect on ice edge position.

The agreement between model and analysis SST suggests that the discrepancy between model and observed ice edge in March, between 52 and 58°N is related to factors other than the position of the SST front. An alternative interpretation is that there are errors in the analysis SST arising from limited spatial and temporal resolution of the satellite data as in February. Between February and March the observed ice edge recedes (compare Figures 5 and 10); the model edge recedes more rapidly. Therefore, an additional reason why assimilation of SST does not correct the ice edge position is because assimilation of SST outside of the ice cover has little impact on receding ice.

6. Model Sensitivity

We noted earlier that because of the weak stratification it was necessary to assimilate surface salinity together with SST. We choose the analysis increment for salinity to be proportional to the analysis increment for temperature according to (7). We now modify the proportionality constant c to examine the sensitivity to this parameter. In Figure 12 we draw a cross-section of salinity along 60°N in mid-March for the assimilation run. In Figure 12a, c is 0.1 (the assimilation run described in the previous section) and in Figure 12b, c is 0.2. In the deep Labrador Sea (east of 59°W) there is a clear difference in the vertical mixing with deeper mixing associated with the smaller c. However in the more stratified water over the shelf and slope the difference is less evident.

In Figure 13 we draw the ice edge for the assimilation run with c = 0.1 and 0.2 and the observed edge on 16 March 1997. The difference between the assimilation runs with the two values of c is negligible south of 55°N. Assimilation of surface salinity, or a procedure with similar effect, is necessary to counteract the buoyancy flux associated with assimilating SST. The greatest effect is on the mixed layer depth in the deep Labrador Sea. Its effect on the ice edge is secondary.

7. Conclusions

We have compared model ice with the observed ice distribution; we have not compared model ocean temperature with in situ measurements. There is no evidence for the assimilation correcting an initial, climatological ocean state. Rather, the changes to ice distribution appear to be most sensitive to the position of the SST front.

In February the ice cover is advancing. The effect of assimilation is to shift the model front to the location of the analysis front with a corresponding shift in the model ice edge. However the shift in model ice edge is away from the observed ice edge.

The failure of the assimilation is related to insufficient spatial and temporal resolution in the winter satellite SST data. Errors in the analysis SST field derive from the sparse data distribution and the assumed form for the background error correlation.

The ice edge in March has retreated inshore from its position in February. Assimilation of SST has little influence on the ice edge because the model and analysis SST agree well; i.e. the discrepancy in ice edge location is not related to errors in the location of the SST front. In addition, assimilation outside the ice cover has little influence on the retreat of ice.

A number of questions remain. For example, how long does the model retain information from the assimilation? How is the surface information transferred to depth?

The assimilation of SST (with the present generation of satellite sensors) has not been shown useful in improving ice edge location. The distribution of satellite SST data is worst in February and March but improves thereafter. Therefore the techniques in this report may have value for model applications (such as iceberg deterioration) which require the position of the SST front later in the year.

References

Anderson, E. and others, 1999. LAPACK Users' Guide, 3rd Edition. Society for Industrial and Applied Mathematics, Philadelphia.

Annan, J. D., and J. C. Hargreaves, 1999. Sea surface temperature assimilation for a three-dimensional baroclinic model of shelf seas. *Cont. Shelf Res., 19*, 1507-1520.

Blumberg, A. F., and G. L. Mellor, 1987. A description of a three-dimensional coastal ocean circulation model, in *Three-Dimensional Coastal Ocean Models, Coastal Estuarine Sci., 4*, edited by N. Heaps, pp. 1-16. AGU Washington, D. C.

Daley, R., 1991. Atmospheric Data Analysis, Cambridge University Press.

Ezer, T., and G. L. Mellor, 1997. Data assimilation experiments in the Gulf Stream region: How useful are satellite-derived data for nowcasting the subsurface fields? *J. Atmos. Oceanic Tech., 14*, 1379-1391.

Fischer, M., and M. Latif, 1995. Assimilation of temperature and sea level observations into a primitive equation model of the tropical Pacific. *J. Mar. Sys.*, 6, 31-46.

Hibler, W. D., 1979. A dynamic thermodynamic sea ice model. *J. Phys. Oceanogr., 9*, 815-846.

Hibler, W. D., 1980. Modeling a variable thickness sea ice cover. *Mon. Wea. Rev., 108*, 1943-1973.

Holland, W. R., and P. Malanotte-Rizzoli, 1989. Assimilation of altimeter data into an ocean model: Space versus time resolution studies. *J. Phys. Oceanogr., 19*. 1507-1534.

Malanotte-Rizzoli, P., and R. E. Young, 1992. How useful are localized clusters of traditional oceanographic measurements for data assimilation? *Dyn. Atmos. Oceans, 17*, 23-61.

Mellor, G. L., 1996. User's guide for a three-dimensional primitive equation, numerical ocean model, 35 pp. Atmospheric and Ocean sciences Program, Princeton University, Princeton, N. J.

Mellor, G. L. and L. Kantha, 1989. An ice-ocean coupled model. *J. Geophys. Res., 94*, 10,937-10,954.

Smith, E., J. Vazquez, A. Tran, and R. Sumagaysay, 1996. Satellite-derived sea surface temperature data available from the NOAA/NASA Pathfinder program. American Geophysical Union, electronic publication, http://www.agu.org/eos_elec/95274e.html.

Tang, C. L., and C. K. Wang, 1996. A gridded data set of temperature and salinity for the northwest Atlantic Ocean, *Can. Data Rep. Hydrogr. Ocean Sci., 148*, 45 pp.

Yao, T., C. L. Tang, and I. K. Peterson, 2000. Modeling the seasonal variation of sea ice in the Labrador Sea with a coupled multi-category ice model and the Princeton Ocean Model. *J. Geophys. Res., 105*, 1153-1165.

Table 1. Assimilation parameters

Parameter and equation	Value
L (3)	500 km
L_h (3)	500 m
ε_O^2 (1)	1
R (5)	20 m / 1 day
c (7)	0.1 $°C^{-1}$

Table 2. Rms SST difference (°C), model – Pathfinder

	Control	Assimilation
February	1.65	0.96
March	1.60	0.98

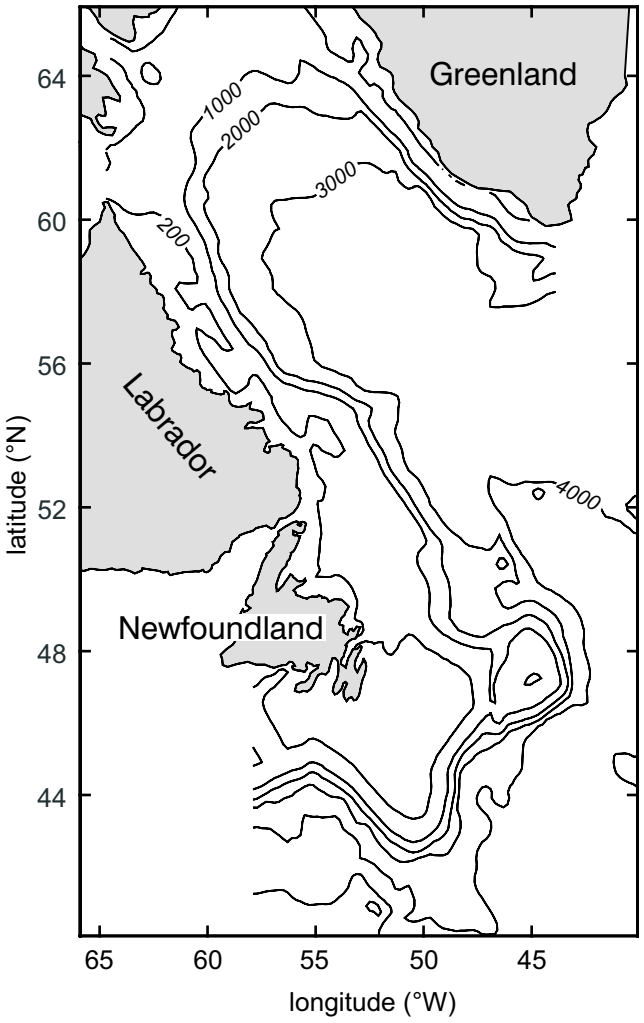

Figure 1. The model domain. Depth contours are in m.

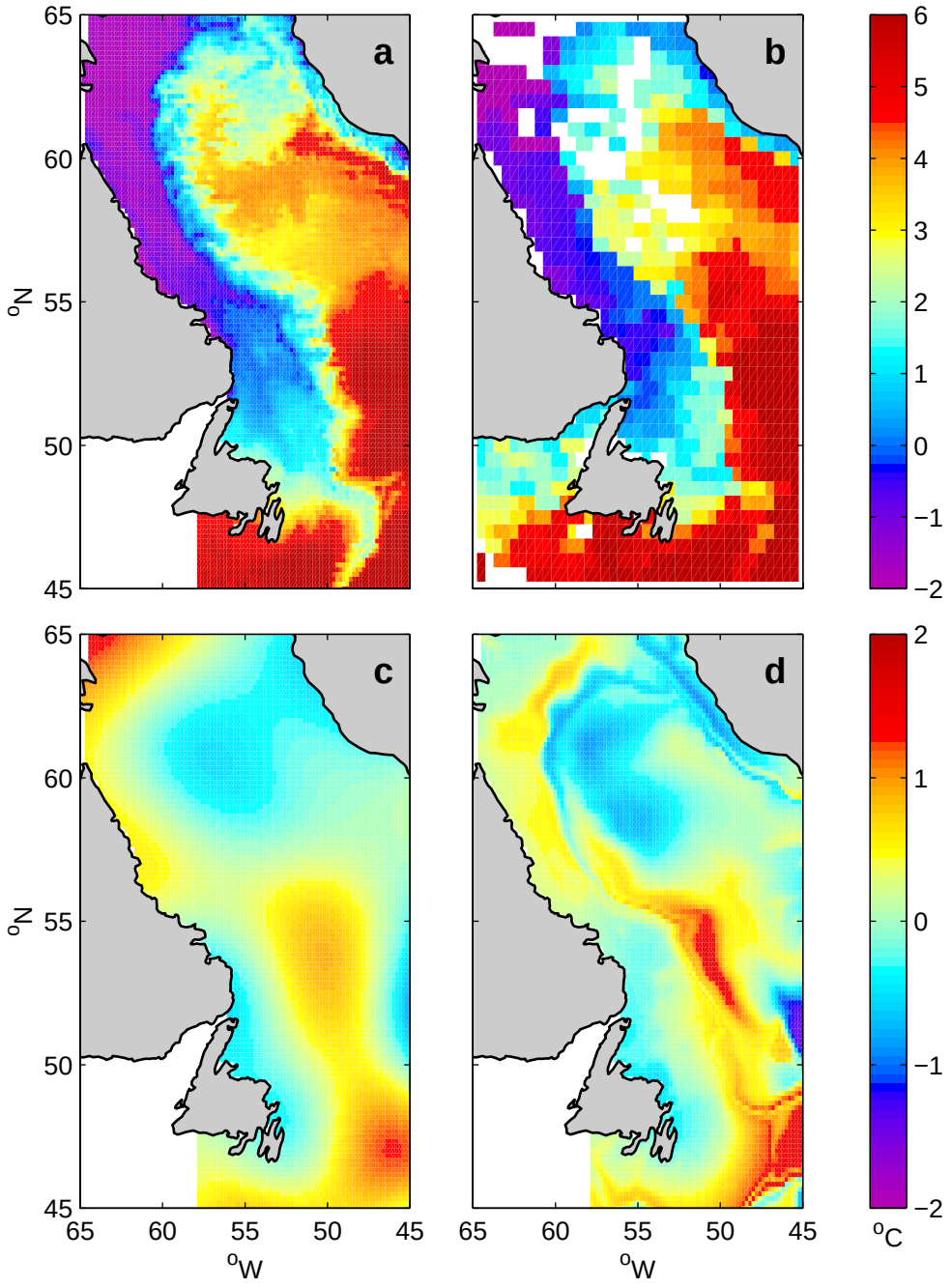

Figure 2. a) SST on 15 December 1996 from control run. b) Pathfinder SST monthly average, December 1996. c) Analysis increment derived from a and b omitting depth-dependent term in background correlation. d) Analysis increment including depth-dependent term in background correlation.

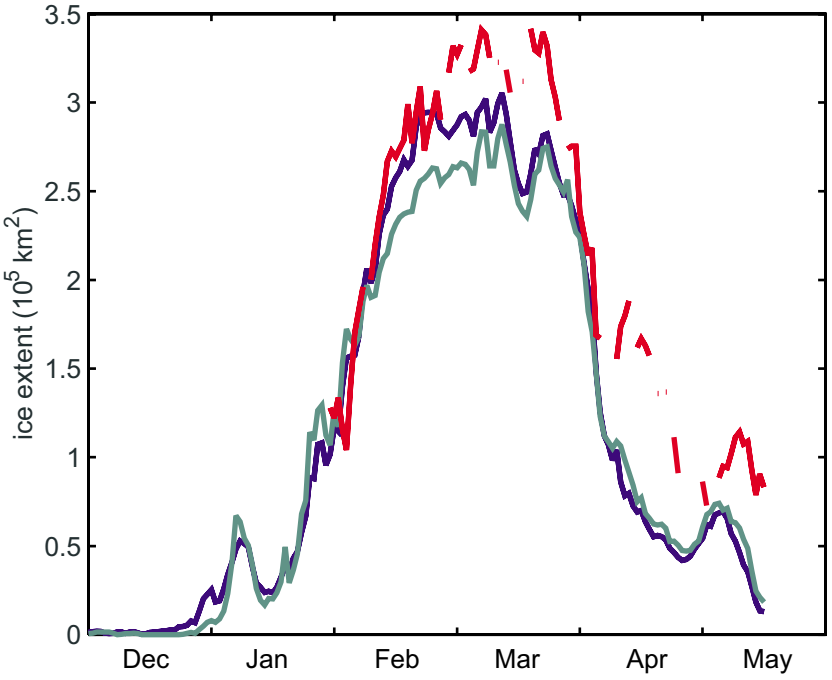

Figure 3. Sea ice extent south of 55°N for control run (blue), assimilation run (green), and observed ice (red).

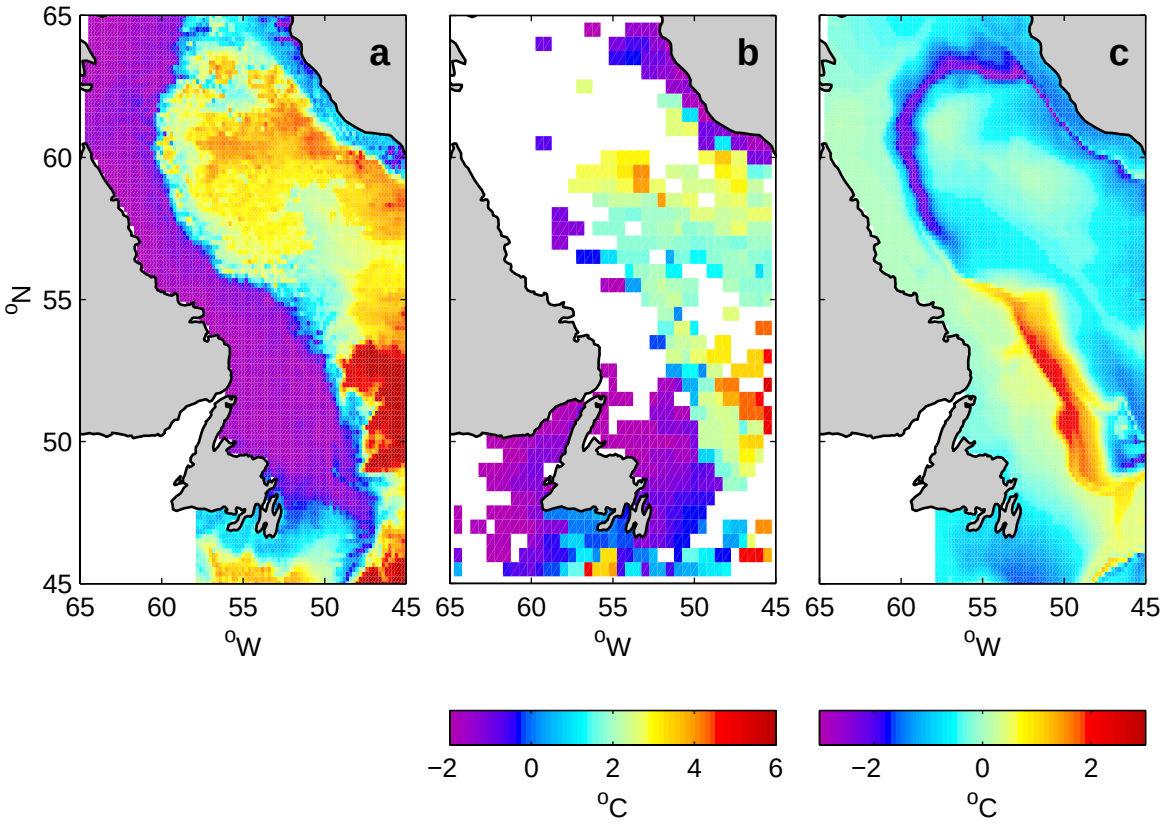

Figure 4. a) SST on 13 February 1997 from control run. b) Pathfinder SST monthly average, February 1997. c) Analysis increment from a and b.

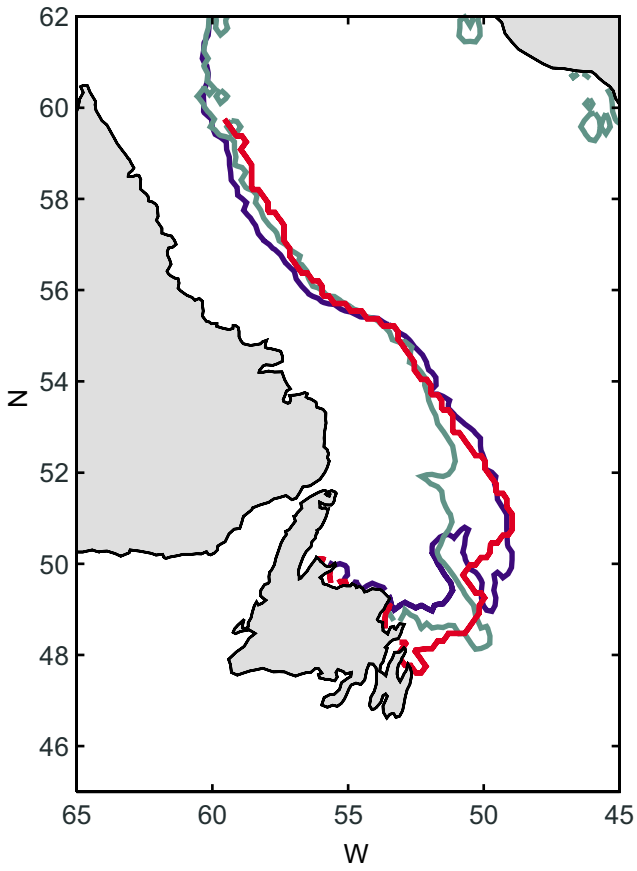

Figure 5. Ice edge on 13 February 1997 for control run (blue), assimilation run (green), and observed ice (red).

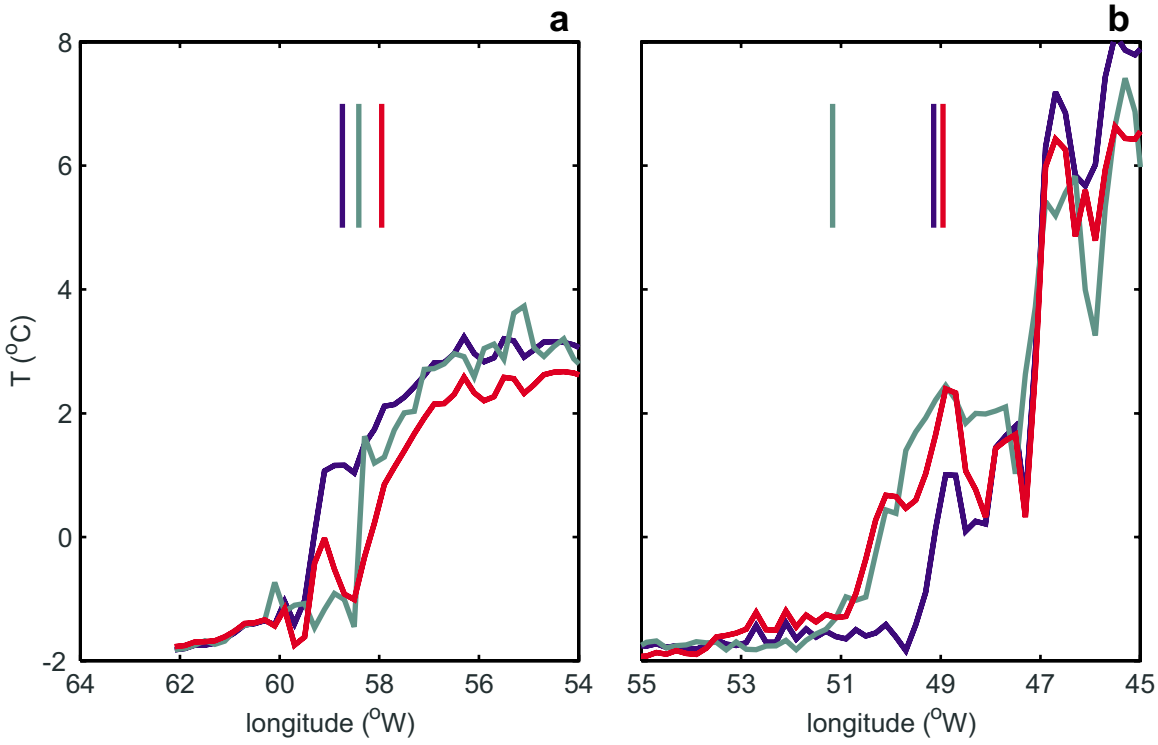

Figure 6. Cross-sections of SST along a) 58°N and b) 51°N on 13 February 1997 for control run (blue), assimilation run (green), and analysis SST (red) derived from control run and February Pathfinder data. The vertical lines are the ice edge location for the control run (blue), assimilation run (green), and observed ice (red).

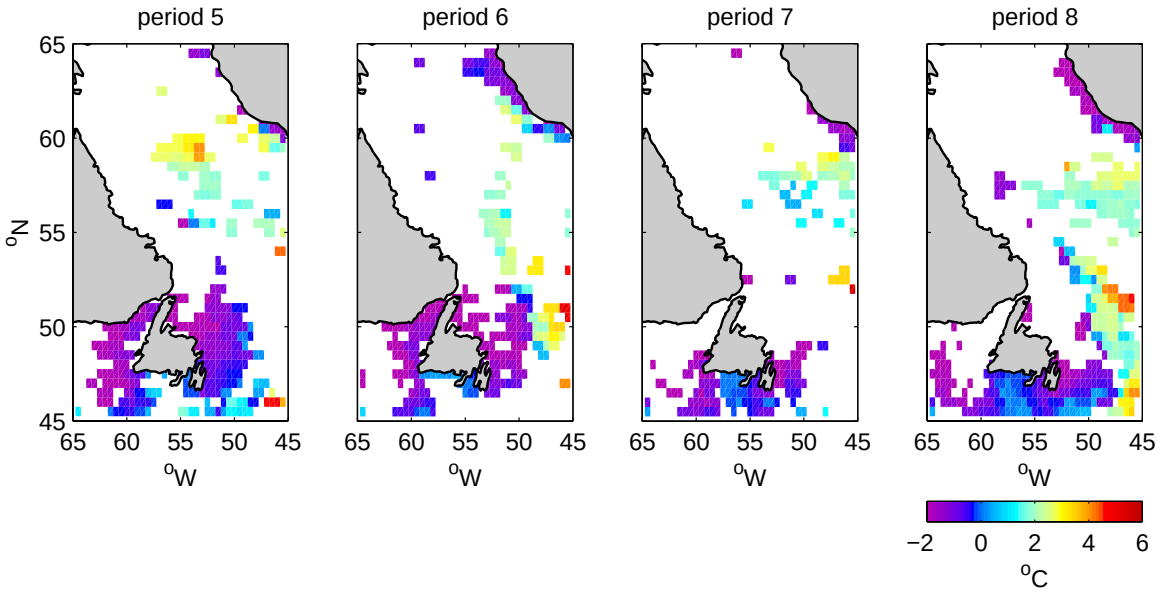

Figure 7. Pathfinder SST data for the four 8-day periods spanning February 1997.

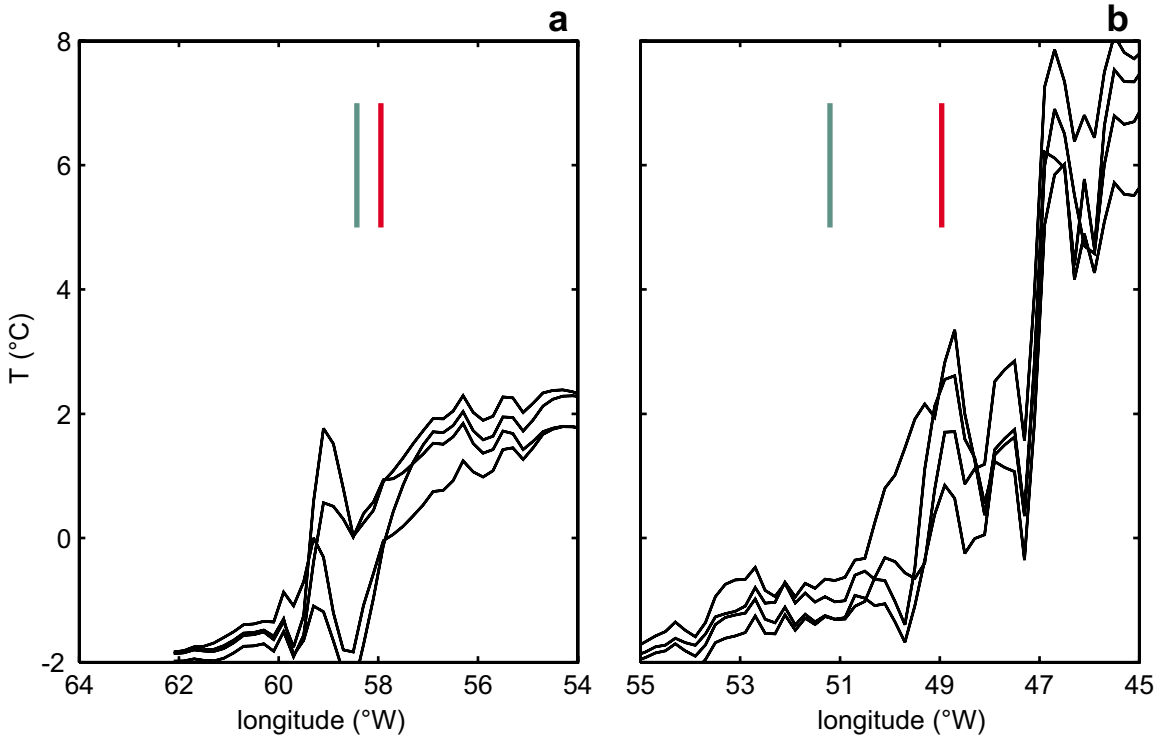

Figure 8. Cross sections of analysis SST along a) 58°N and b) 51°N derived from mid-February control run and each of the four 8-day Pathfinder SST data fields in February. The vertical lines are the ice edge locations for the assimilation run (green) and the observed ice (red).

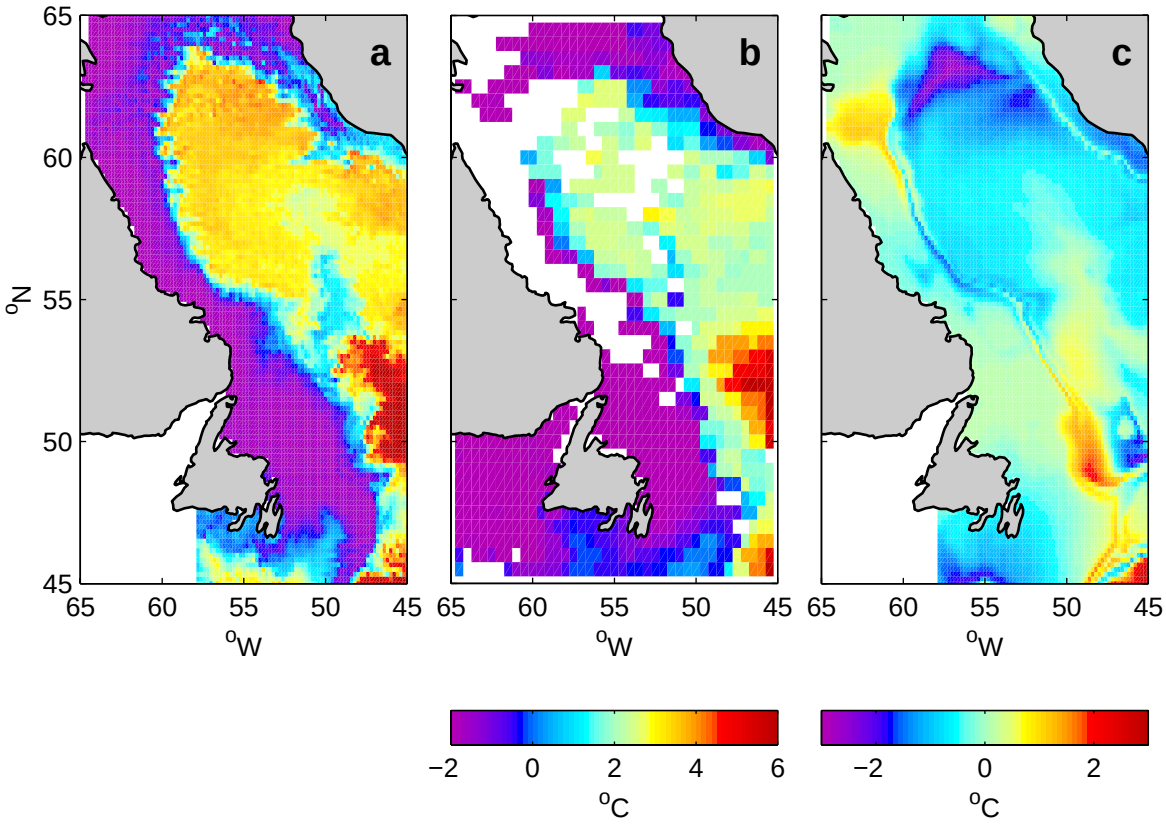

Figure 9. a) SST on 16 March 1997 from control run. b) Pathfinder SST monthly average, March 1997. c) Analysis increment from a and b.

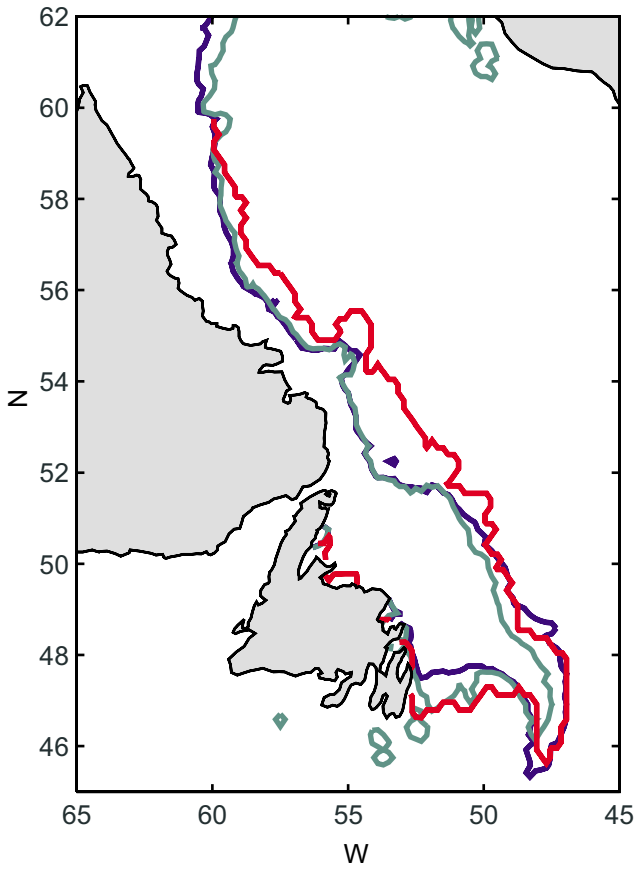

Figure 10. Ice edge 16 March 1997 for control run (blue), assimilation run (green), and observed ice (red).

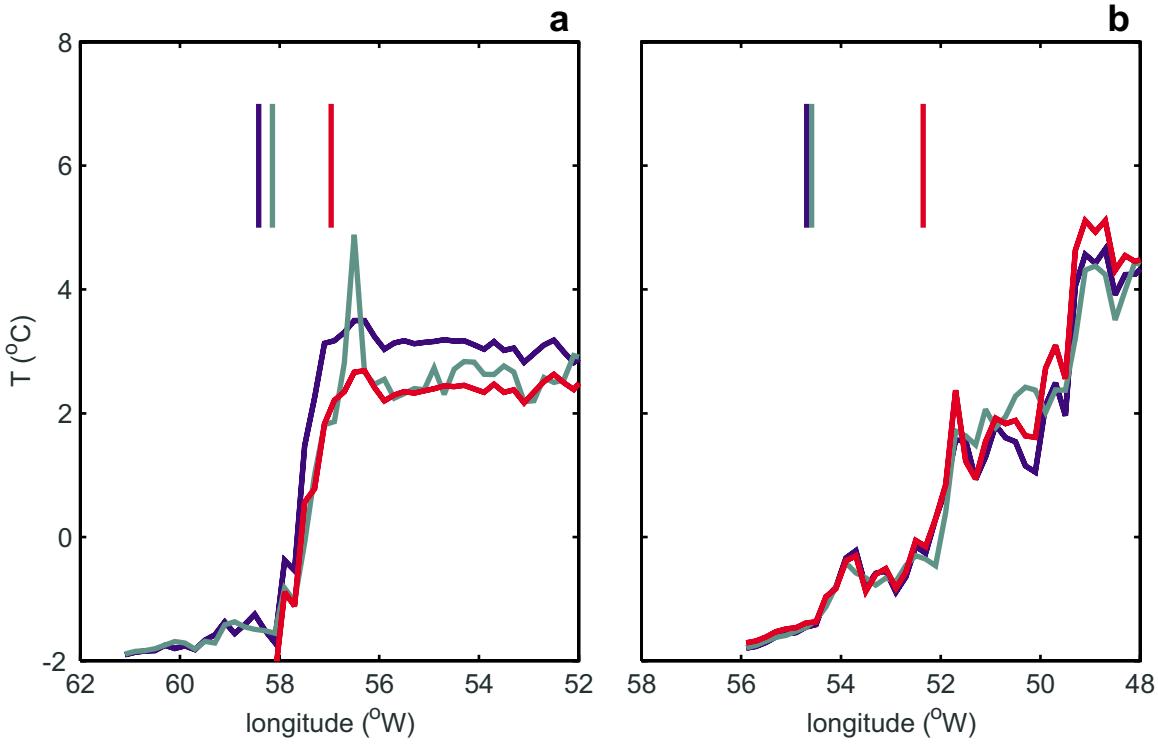

Figure 11. Cross-sections of SST along a) 56°N and b) 53°N on 16 March 1997 for control run (blue), assimilation run (green), and analysis SST (red) derived from control run and March Pathfinder data. The vertical lines are the ice edge locations for the control run (blue), assimilation run (green), and observed ice (red).

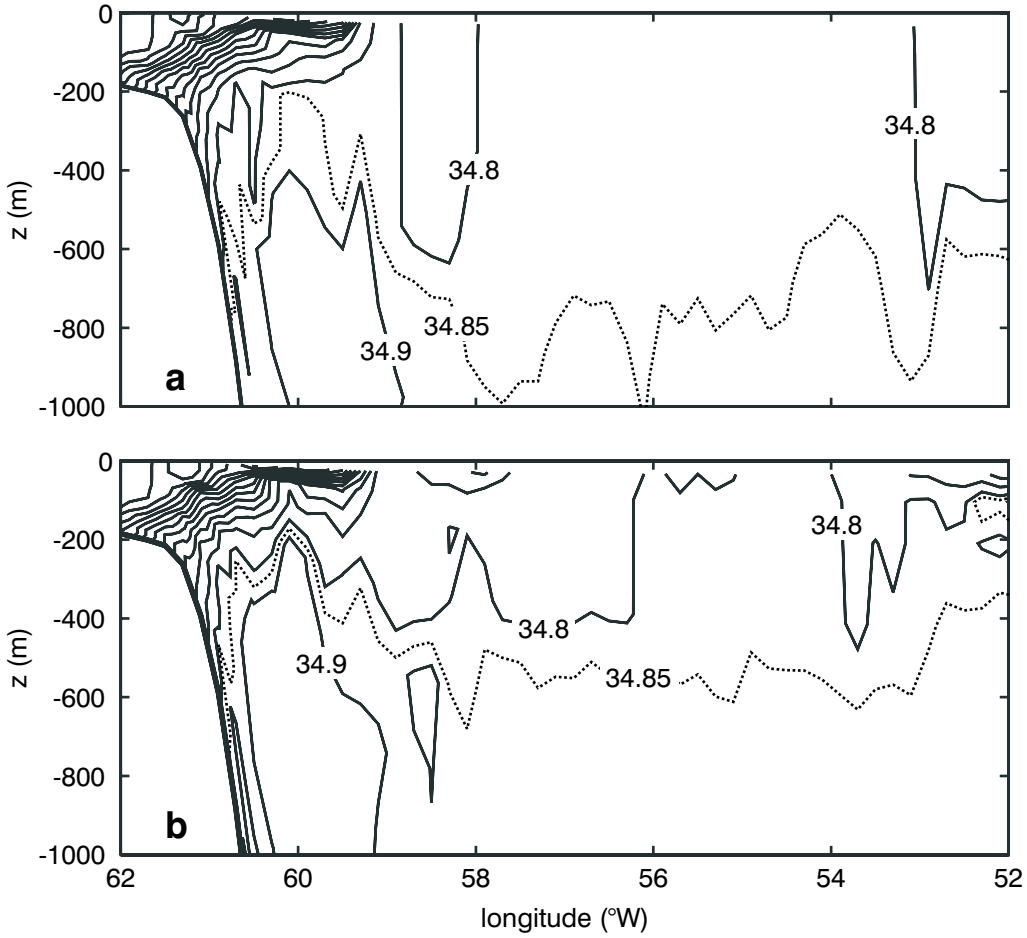

Figure 12. Cross section of salinity along 60°N, mid-March from assimilation run with a) parameter c = 0.1 and b) c = 0.2. The contour interval is 0.1 with the additional contour level 34.85 drawn.

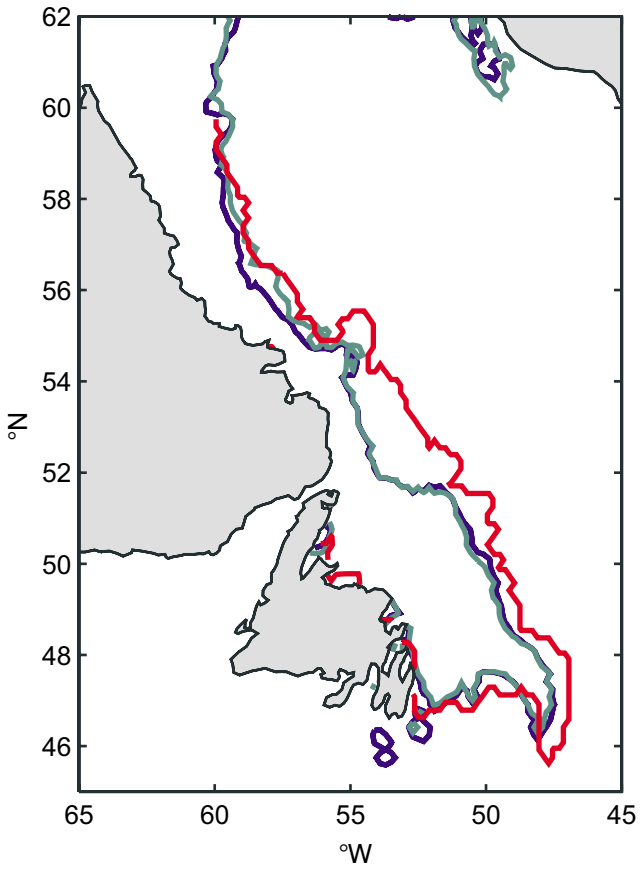

Figure 13. Ice edge on 16 March 1997 for assimilation run with c = 0.1 (blue), c = 0.2 (green), and observed ice (red).